J. Marine Sci. Appl. (2012) 11: 18-23
DOI: 10.1007/s11804-012-1101-x

Multi-domain Boundary Element Method with Dissipation

Xiaobo Chen[1,2*] and Wenyang Duan[3]

1. Research Department, Bureau Veritas, Neuilly-Sur-Seine 92571, France
2. The University of Western Australia, Perth, Australia
3. Shipbuilding Engineering College, Harbin Engineering University, 150001 Harbin, China

Abstract: The wave diffraction and radiation around a floating body is considered within the framework of the linear potential theory in a fairly perfect fluid. The fluid domain extended infinitely in the horizontal directions but is limited by the sea bed, the body hull, and the part of the free surface excluding the body waterplane, and is subdivided into two subdomains according to the body geometry. The two subdomains are connected by a control surface in fluid. In each subdomain, the velocity potential is described by using the usual boundary integral representation involving Green functions. The boundary integral equations are then established by satisfying the boundary conditions and the continuous condition of the potential and the normal derivation across the control surface. This multi-domain boundary element method (MDBEM) is particularly interesting for bodies with a hull form including moonpools to which the usual BEM presents singularities and slow convergence of numerical results. The application of the MDBEM to study the resonant motion of a water column in moonpools shows that the MDBEM provides an efficient and reliable prediction method.
Keywords: multi-domain boundary element method (MDBEM); fairly perfect fluid; moonpool resonance; dissipation
Article ID: 1671-9433(2012)01-0018-06

1 Introduction

A floating body without forward speed on the free surface and in the presence of incident propagative waves is considered. The reference system of Cartesian coordinates is defined by letting the (x, y) plane coincide with the mean free surface and z-axis be positive upwards so that

$$z=\zeta(x, y, t) \tag{1}$$

describes the elevation of the free surface. The fluid is assumed to be incompressible and inviscid while the fluid motion is irrotational. Under these assumptions of a perfect fluid, the flow velocity $\boldsymbol{V}=(V_1, V_2, V_3)$ can be expressed as the gradient of a scalar potential $\Phi(M, t)$ in the space $M=(x, y, z)$ at the time t:

$$\boldsymbol{V}=\nabla\Phi$$

The mass conservation law is described by:

$$\nabla\cdot\boldsymbol{V}=0 \qquad \text{then} \qquad \nabla^2\Phi=0 \tag{2}$$

showing that the Laplace equation is satisfied by the velocity potential. The fluid is under the action of gravity. Besides this gravitational field, an internal force defined as

$$\boldsymbol{f}=-\mu\boldsymbol{V} \tag{3}$$

is assumed to apply to the fluid particle as well. The parameters μ being assumed to be positive and small, the force $\boldsymbol{f}$ is proportional to the magnitude of fluid velocity but in the opposite direction. Although $\boldsymbol{f}$ plays the same role of damping fluid motion and dissipating energy as that of fluid viscosity, it does not introduce any vorticity so that the existence of the velocity potential is safeguarded. The inviscid and irrotational fluid with the dissipative force $\boldsymbol{f}$ is regarded here as a fairly perfect fluid in Guével (1982) and Chen (2004).

The momentum equation in the fairly perfect fluid is written as:

$$(\partial/\partial t+\boldsymbol{V}\cdot\nabla)\boldsymbol{V}=-\nabla(P/\rho+gz)-\mu\boldsymbol{V} \tag{4}$$

in which P stands for the pressure and g the gravitational acceleration. Introducing $\boldsymbol{V}=\nabla\Phi$ into above momentum equation, the modified Bernoulli equation is obtained and expressed as:

$$P/\rho+gz+\Phi_t+\nabla\Phi\cdot\nabla\Phi/2+\mu\Phi=C(t) \tag{5}$$

with $C(t)$ an arbitrary function of t usually omitted by redefining Φ without affecting the velocity field. The Bernoulli Eq.(5) provides the pressure in the fluid:

$$P=-\rho(gz+\Phi_t+\nabla\Phi\cdot\nabla\Phi/2+\mu\Phi) \tag{6}$$

On the free surface $z=\zeta$, the dynamic condition requires that the pressure given from (6) is equal to the atmospheric pressure ($P=0$), i.e.

$$gz+\Phi_t+\nabla\Phi\cdot\nabla\Phi/2+\mu\Phi=0 \tag{7}$$

which gives the free-surface elevation by putting $z=\zeta$:

$$\zeta=-(\Phi_t+\nabla\Phi\cdot\nabla\Phi/2+\mu\Phi)/g \tag{8}$$

Since Eq.(7) holds for all time at the free surface $z=\zeta$, its material derivative $(\partial_t+\nabla\Phi\cdot\nabla)$ must be set equal to zero

Received date: 2011-10-26.
***Corresponding author Email:** xiao-bo.chen@bureauveritas.com

and is shown as :

$$\begin{aligned} &\Phi_{tt} + g\Phi_z + \mu\Phi_t + 2\nabla\Phi\cdot\nabla\Phi_t + \\ &\nabla\Phi\cdot\nabla(\nabla\Phi\cdot\nabla\Phi)/2 + \mu\nabla\Phi\cdot\nabla\Phi = 0 \end{aligned} \tag{9}$$

Furthermore, a particle in motion at the free surface stays always on the same surface. This kinematic condition is expressed by the material derivative of (1) with respect to the time, i.e.

$$\Phi_z - \Phi_x\zeta_x - \Phi_y\zeta_y - \zeta_t = 0 \tag{10}$$

on the exact free surface $z = \zeta$.

In the presence of a body, the boundary condition on body's hull is expressed by the fact that the normal velocity of the fluid is equal to that of the body at a point on the hull:

$$\Phi_n = \boldsymbol{V}^E\cdot\boldsymbol{n} \tag{11}$$

where $\boldsymbol{V}^E$ stands for the local velocity vector of body's hull. If the sea bed $B(z = -h)$ is present, an additional condition

$$\Phi_z = 0 \tag{12}$$

is written on B.

The above boundary value problem can be linearized in relation to the mean position of boundaries. The linearized boundary value problem is then solved by applying Green's identity which permits expression of the velocity potential by the integral representation involving the potential and its normal derivative on the boundaries. The satisfaction of the boundary conditions yields the integral equation of which the solution gives the potential distribution.

The above boundary element method (BEM) is summarized in this paper with application to the wave radiation and diffraction around a floating body. Unlike the usual BEM, a dissipation force (3) is introduced in the momentum equation (4). The boundary condition at the free surface involves an additional term associated with the dissipation coefficient. The boundary integral at the free surface is no longer nil although that the Green function satisfies the linear free-surface condition is used.

The fluid domain extended infinitely in the horizontal directions but limited by the sea bed, the body hull, and the part of free surface excluding the body waterplane is subdivided into two subdomains according to the body geometry. The two subdomains are connected by a control surface in fluid. In each subdomain, the velocity potential is described by using the usual boundary integral representation involving Green functions. The boundary integral equations are then established by satisfying the boundary conditions and the continuous condition of the potential and the normal derivation across the control surface.

This multi-domain boundary element method (MDBEM) is particularly interesting for bodies with special hull forms including moonpools to which the usual BEM presents singularities and slow convergence of numerical results. The application of the MDBEM to study the resonant motion of water columns in moonpools shows that the MDBEM provides an efficient and reliable prediction method.

2 BEM with dissipation

By assuming a small steepness of incident waves, the linearization of the above equations is used. Furthermore, the fluid motion is assumed to be harmonic in time with the circular frequency ω in such a way that the velocity potential

$$\Phi(M, t) = \mathrm{Re}\{\,\phi(M)\ \mathrm{e}^{-\mathrm{i}\omega t}\,\} \tag{13}$$

can be written. In (13), $\mathrm{Re}\{\cdot\}$ stands for taking the real part. The linear problem of wave radiation is then defined by:

$$\nabla^2\phi = 0 \qquad M \subset D \tag{14a}$$

$$\phi_z - K_0(1+\mathrm{i}\varepsilon)\phi = 0 \qquad M \subset F \tag{14b}$$

$$\phi_n = v_n \qquad M \subset H \tag{14c}$$

$$\phi_z = 0 \qquad M \subset B \tag{14d}$$

in which $K_0 = \omega^2/g$ and $\varepsilon = \mu/\omega$, D stands for the fluid domain limited by the mean free-surface F, the body surface H, the sea bed B, and a cylindrical surface C^∞ ($x^2+y^2 \to \infty$) at the infinity. The so-called radiation condition requiring that φ disappears on C^∞ is satisfied automatically in the fairly perfect fluid. The term v_n on the right hand side of (14c) is a given function following the radiation and diffraction problems.

To solve the first-order boundary value problem defined by (14), one fundamental solution which satisfies the following equations is considered:

$$\nabla^2 G(M,Q) = 4\pi\delta_{MQ} \qquad M \subset D \tag{15a}$$

$$G_z - K_0(1+\mathrm{i}\varepsilon)G = 0 \qquad M \subset F \tag{15b}$$

$$G_z = 0 \qquad M \subset B \tag{15c}$$

in which (M, Q) are respectively the field point $M(x, y, z)$ and singular point $Q(x', y', z')$, and the Dirac function $\delta_{MQ} = \delta(x-x')\delta(y-y')\delta(z-z')$. In principle, the parameter ε' involved in the free-surface boundary condition (15b) takes the same value as ε in (14b). However, it may be different from ε which can even be variable depending on the zone of free surface. Such a solution is called the Green function representing the field of velocity potential at $M(x, y, z)$ created by a source of unit density located at $Q(x', y', z')$. Applying Green's second formula to the two harmonic functions (Φ, G), we have:

$$4\pi\phi(M) = \iint_{\partial D} \mathrm{d}s[\phi_n(Q)G(M,Q) - \phi(Q)G_n(M,Q)] \tag{16}$$

in which the normal vector $\boldsymbol{n}$ is oriented positively toward

into fluid. The left hand side is the result of the domain integral while the terms on the right side come from the transformation of the domain integral to the surface integral on the boundaries according to the formula of Ostrogradsky. The boundary surfaces ∂D include the ship's hull H, the mean free surface F the sea bed B, and a surface at infinity C^∞:

$$\partial D = H \bigcup F \bigcup B \bigcup C^\infty$$

The integral on the surface at infinity C^∞ is nil in a fluid with dissipation. The integral over the sea bed is nil as well. The Eq.(16) is then reduced to:

$$4\pi\phi(M) = \iint_H \mathrm{d}s(\phi_n G - \phi G_n) - \mathrm{i}K_0 \iint_F \mathrm{d}s(\varepsilon - \varepsilon')\phi G \quad (17)$$

for $M \subset D$, in which the integral over the free surface is evaluated by making use of (14b) and (15b). This free surface integral is simplified or equal to zero in most cases of wave radiation and diffraction without forward speed where there has been traditionally ε=0=ε', or can be transformed into a line integral for the wave radiation and diffraction around an advancing ship at a uniform speed.

In the case when ε'=0 in (15b) for $G(M, Q)$, the integral Eq.(17) can be written directly

$$2\pi\phi + \mathrm{PV}\iint_H \mathrm{d}s\phi G_n + \mathrm{i}K_0 \iint_F \mathrm{d}s\varepsilon\phi G = \iint_H \mathrm{d}s v_n G \quad (18a)$$

for $M \subset H$ and

$$4\pi\phi + \iint_H \mathrm{d}s\phi G_n + \mathrm{i}K_0 \iint_F \mathrm{d}s\varepsilon\phi G = \iint_H \mathrm{d}s v_n G \quad (18b)$$

for $M \subset F$. In (18a), $\mathrm{PV}\iint$ stands for taking the Cauchy principal value of the integral.

The integral over the free surface F depends on the value of ε; in other words, only the part of the free surface $\overline{F}$ over which $\varepsilon \neq 0$ is involved in the integral Eqs.(18) because of the integration over the remaining part where ε=0. In the following application, it is necessary only to put non-zero ε over the free surface contained by the moonpool in which the fluid kinematics is resonant.

3 Multi-domain BEM

As illustrated on Fig.1, the fluid domain D is divided into an interior domain D^I and an exterior D^E subdomain which are surrounded by their boundaries respectively.

$$\partial D^I = H^I \bigcup F^I \bigcup C^I \bigcup B^I$$
$$\partial D^E = H^E \bigcup F^E \bigcup C^E \bigcup B^E \bigcup C^\infty$$

The surfaces (H^I, H^E) are parts of the body hull belonging to the subdomains (D^I, D^E), i.e. H=$H^I \cup H^E$. The same for F=$F^I \cup F^E$. The control surfaces (C^I, C^E) are the two sides of the same control surface C:

$$C^I = C = C^E \qquad \text{but} \qquad \boldsymbol{n}(C^I) = \boldsymbol{n}(C) = -\boldsymbol{n}(C^E)$$

Finally, the surface C^∞ is at infinity and the Green integral over it is supposed to disappear.

The potentials in the interior and exterior subdomains can be represented by the Green integrals similar to (17):

$$4\pi\phi^I = \iint_{H^I} \mathrm{d}s(v_n^I G - \phi^I G_n) - \mathrm{i}K_0 \iint_{F^I} \mathrm{d}s\varepsilon\phi^F G + \iint_C \mathrm{d}s(\varphi^C G - \phi^C G_n) \quad (19a)$$

for $M \subset D^I$ and

$$4\pi\phi^E = \iint_{H^E} \mathrm{d}s(v_n^E G - \phi^E G_n) - \iint_C \mathrm{d}s(\varphi^C G - \phi^C G_n) \quad (19b)$$

for $M \subset D^E$.

In (19), the boundary conditions (ϕ_n^I, ϕ_n^E) = (v_n^I, v_n^E) are used in the integrals on (H^I, H^E), respectively, while $\varphi^C = \phi_n^C$ on C^I is used in both integrals on C^I and C^E.

The unknown distributions of ϕ^I on H^I, ϕ^E on H^E, both φ^C and ϕ^C on C, and ϕ^F on F^I are determined by the integral equations as follows:

$$2\pi\phi^I + \mathrm{PV}\iint_{H^I} \mathrm{d}s\phi^I G_n - \iint_C \mathrm{d}s(\varphi^C G - \phi^C G_n) + \mathrm{i}K_0 \iint_{F^I} \mathrm{d}s\varepsilon\phi^F G = \iint_{H^I} \mathrm{d}s v_n^I G \quad (20a)$$

for $M \subset H^I$

$$2\pi\phi^E + \mathrm{PV}\iint_{H^E} \mathrm{d}s\phi^E G_n + \iint_C \mathrm{d}s(\varphi^C G - \phi^C G_n) = \iint_{H^E} \mathrm{d}s v_n^E G \quad (20b)$$

for $M \subset H^E$

$$4\pi\phi^C + \iint_{H^I} \mathrm{d}s\phi^I G_n + \iint_{H^E} \mathrm{d}s\phi^E G_n + \mathrm{i}K_0 \iint_{F^I} \mathrm{d}s\varepsilon\phi^F G = \iint_{H^I} \mathrm{d}s v_n^I G + \iint_{H^E} \mathrm{d}s v_n^E G \quad (20c)$$

for $M \subset C$

$$4\pi\varphi^C + \iint_{H^I} \mathrm{d}s\phi^I \partial_n G_n + \iint_{H^E} \mathrm{d}s\phi^E \partial_n G_n + \mathrm{i}K_0 \iint_{F^I} \mathrm{d}s\varepsilon\phi^F \partial_n G = \iint_{H^E} \mathrm{d}s v_n^E \partial_n G + \iint_{H^I} \mathrm{d}s v_n^I \partial_n G \quad (20d)$$

for $M \subset C$ and

$$4\pi\phi^F + \iint_{H^I} \mathrm{d}s\phi^I G_n - \iint_C \mathrm{d}s(\varphi^C G - \phi^C G_n) + \mathrm{i}K_0 \iint_{F^I} \mathrm{d}s\varepsilon\phi^F G = \iint_{H^I} \mathrm{d}s v_n^I G \quad (20e)$$

for $M \subset F^I$, respectively.

The integral Eqs.(20c) and (20d) are derived from the continuous conditions

$$\phi^I = \phi^E \qquad \text{and} \qquad \phi_n^I = \phi_n^E \quad (21)$$

across the control surface C and the normal direction on the side C^I being used. The continuous conditions (21) have been implicitly used in (19).

In the integral Eq.(20) of MDBEM, the derivatives of the Green function are understood as:

$$G_n = \partial G(M, Q) / \partial n(Q) \quad (22a)$$

$$\partial_n G = \partial G(M,Q)/\partial n(M) \tag{22b}$$

$$\partial_n G_n = \partial[\partial G(M,Q)/\partial n(Q)]/\partial n(M) \tag{22c}$$

The integration of the second derivatives Eq.(22c) of the Green function associated with its Rankine part is hypersingular and must be evaluated as a Hadamard finite-part integral.

4 Hydrodynamic loading

The time-harmonic potential defined by (14) is further expressed as the sum of various components:

$$\phi = -\mathrm{i}\omega\sum_{j=1}^{6} a_j\phi_j + a_0(\phi_0+\phi_7) \tag{23}$$

in which $\phi_{1,2,\cdots,6}$ are radiation potentials corresponding to 6 degree of freedom oscillations of the body and $a_{1,2,\cdots,6}$ are the amplitudes of corresponding motions. ϕ_0 is the potential of incoming waves and is given by

$$\phi_0 = -\frac{g}{\omega}\frac{\cosh k_0(z+h)}{\cosh k_0 h}\mathrm{e}^{\mathrm{i}k_0(x\cos\beta+y\sin\beta)} \tag{24}$$

while ϕ_7 is the potential due to the diffracted waves associated with the amplitude a_0 of incoming waves. In (24), β is the wave heading and the wave number k_0 determined by the dispersion relationship:

$$k_0\tanh k_0 h = K_0 = \omega^2/g \tag{25}$$

The terms v_n in the hull integral on the right hand side of (18) and (20) associated with the radiation and diffraction potentials ϕ_j defined in (23) for j = 1, 2,⋯, 7 is given by:

$$v_n = \begin{cases} n_j & j=1,2,\cdots,6 \\ -\partial\phi_0/\partial n & j=7 \end{cases} \tag{26}$$

In (26), the generalized vector (n_1, n_2 , ⋯ , n_6) is defined as:

$$(n_1,n_2,n_3) = \boldsymbol{n} \quad \text{and} \quad (n_4,n_5,n_6) = \boldsymbol{r}\wedge\boldsymbol{n}$$

in which $\boldsymbol{r}$ = (x–x_0, y –y_0, z –z_0) with O(x_0, y_0, z_0) as the reference point of rotation

Once the integral Eq.(18) is solved, the free surface elevation is then given by

$$\eta = \mathrm{i}\omega(1+\mathrm{i}\varepsilon)\phi/g \tag{27a}$$

evaluated at z=0, while the first-order time-harmonic pressure can be evaluated by

$$P = -\rho g X_3 + \rho\mathrm{i}\omega(1+\mathrm{i}\varepsilon)\phi \tag{27b}$$

with X_3 as the vertical displacement of the body.

The integration of the first term ($\rho g X_3$) in 27(b) plus the variation of gravity load (moments) gives the hydrostatic stiffness C_{ij}. The second term in (27b) yields two parts: the added-mass coefficients (A_{kj}) and damping coefficients (B_{kj}), which are defined by integration of the pressure due to radiation waves:

$$\omega^2 A_{kj} + \mathrm{i}\omega B_{kj} = \omega^2(1+\mathrm{i}\varepsilon)\rho\iint_H \mathrm{d}s\phi_j n_k \tag{28a}$$

and wave exciting loads F_k which are defined by integration of the pressure due to incoming and diffracted waves:

$$F_k = -\mathrm{i}\omega(1+\mathrm{i}\varepsilon)\rho a_0\iint_H \mathrm{d}s(\phi_0+\phi_7)n_k \tag{28b}$$

Finally, the motion amplitude of floating bodies is evaluated by solving the motion equation:

$$\sum_{j=1}^{6}[-\omega^2(M_{kj}+A_{kj}) - \mathrm{i}\omega B_{kj} + C_{kj} + C'_{kj}]a_j = F_k \tag{28c}$$

in which M_{kj} and C'_{kj} for k, j = 1, 2,⋯, 6 are the inertia and additional stiffness matrices, respectively.

5 Water-column motion in moonpool

A hollow structure with an opening at the bottom is one of devices designed to extract wave energy associated with large motions of the water column inside the moonpool. This oscillating water column (OWC) device of axisymmetric cylinder is illustrated on Fig.1.

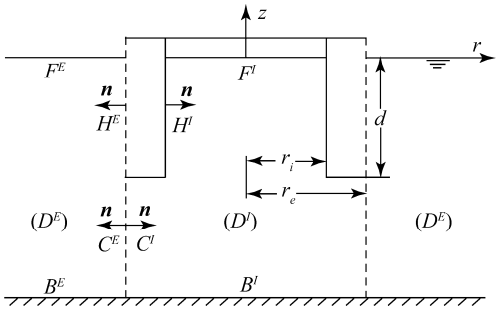

Fig.1 Scheme of moonpool and subdomains

The model tests presented in Sadó Garriga and Falzarano (2004) were performed with a fixed cylinder (open at both ends) of the interior/exterior radii (r_i/r_e) equal to 15.161/16.193 in meters using a scale of 1:100. The cylinder draft is d=76.200 m and the waterdepth h = 198.120 m.

The free-surface elevation at the center of the moonpool is evaluated by using (27a) after having obtained the diffraction solution via the integral Eqs.(18). The dissipation coefficient ε is set to zero as in a usual BEM. One coarse mesh (M1) composed of 620 flat panels is constructed by dividing the circumference by 20 segments, the height by 15 segments and 1 in thickness. Doubling the number of segments in the circumference, height and thickness gives a fine mesh (M2) with 2480 flat panels. Quadrupling the number of segments in the circumference, height, and thickness gives the finest mesh (M3) with 9920 flat panels.

The results using the three meshes (M1, M2, M3) are represented on Fig.2 by the solid, dashed, and dot-dashed lines, respectively. The free-surface elevation scaled with the incoming wave amplitude is depicted in a function of wave periods. The results using the M1 mesh peak at 17.699 seconds while those using (M2, M3) meshes peak at (18.897, 19.883) seconds, respectively. Furthermore, the values at peaks vary from about 40 to 70. The finer the mesh, the higher the peak value.

The results represented in Fig.2 are obtained by the integral Eqs.(18) which is often called potential formulation or direct formulation since the potential is directly related to the solution. There is another formulation called source formulation or indirect formulation since the potential is written as an integration of source distribution which is obtained by solving the associated integral equations. The computations by the source formulation using the same meshes also give the non-convergent results. The peaks of water-column motions in a moonpool are located at different wave periods varying from 8.491 seconds for M1 mesh, 9.378 seconds for M2 mesh, and 10.927 seconds for M3 mesh. In the same way, the peak amplitudes vary for different meshes. The results are manifestly not convergent. This confirms the analysis in Martin and Risso (1993) that the standard integral Eqs.(18) used in usual BEM are degenerate when the body has parts of the hull which are thin.

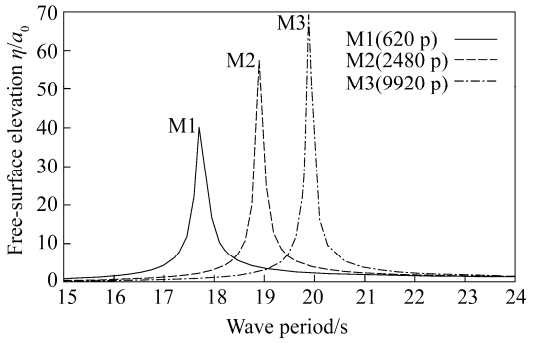

Fig.2 Results of usual BEM with different meshes

The integral Eq.(20) of MDBEM have been implemented in HydroStar of which the theoretical background can be found in Chen (2004). The panels of hull meshes are separated into two groups to be attributed to the interior and exterior domains. This division and the definition of associated control surface are not unique. One type consists to have only the exterior wall as H^E and the control surface (C1) defined as the vertical extension from the bottom of H^E to the sea bed as illustrated on Fig.3. The control surface in the lower part of the figure is represented by wire- frames. Another is to have only the interior wall as H^I and the control surface (C2) defined as the vertical extension from the bottom of H^I to the sea bed. The third type is to have the interior wall as H^I and the control surface (C3) as simply the circular surface to occupy the bottom opening of the moonpool.

The first analysis concerns the results from three ways to subdivide the fluid domain. The coarse mesh composed of 620 panels on the body hull is used together with 400 more panels on the (C1) and (C2) control surfaces, and 100 panels on the (C3) control surface. The results using three control surfaces are represented on Fig.4 by the star and circle symbols, and the solid line, respectively. The peaks of the (C1) and (C2) control surfaces are the same with only a negligible shift compared to that of (C3) control surface. Furthermore, the finer mesh with 2480 panels on H and 400 panels on the control surface of (C3) type is used. The results of this finer (C3) mesh have the same peak position at 18.534 seconds and very close to those of the coarse (C3) mesh, with higher peak amplitude for the finer (C3) mesh. This shows that the results from MDBEM are convergent.

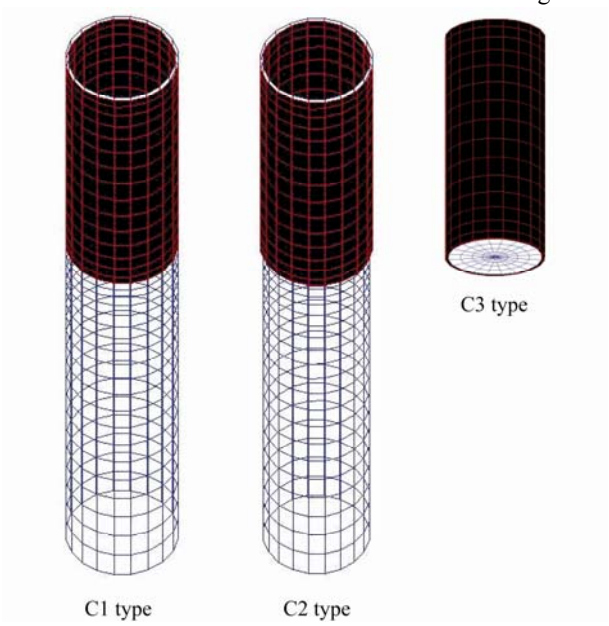

Fig.3 Hull mesh and control surfaces

A number of analyses have been performed to estimate the period of low-frequency resonance of moonpools. The first resonant period (piston mode) can be written as

$$T = 2\pi\sqrt{d(1+\alpha)/g} \tag{29}$$

in which the added-mass coefficient α should be a value greater than 0 by assuming no reaction of fluid below the moonpool bottom to the water-column motion, and $(r_i/d)8/(3\pi)$ = 0.169 due to the maximum reaction by the infinity thickness of moonpools ($r_e \to\infty$), according to the results obtained in Molin (2001) and Newman (2003). The peak period T=18.534 seconds obtained by MDBEM is related to α = 0.120, which is the most likely one.

Finally, the peak amplitude of water-column motion is studied by introducing a non-zero dissipation coefficient in the formulation of MDBEM. The coarse mesh with the control surface of (C3) type is used to compute the free-surface elevation in the center of a moonpool. The

results are depicted in Fig.5 by the solid, dashed, dotted, and dot-dashed lines for the dissipation coefficients ε=0, 0.026, 0.053 and 0.081, respectively. Furthermore, the experimental measurements given in Sadó Garriga and Falzarano (2004) are reported as the square symbols. The introduction of the dissipation force in the fluid yields low peak amplitude in the small zone around the resonant period and negligible effect outside of the resonant zone. As expected, lower peak amplitude is obtained with a larger dissipation coefficient.

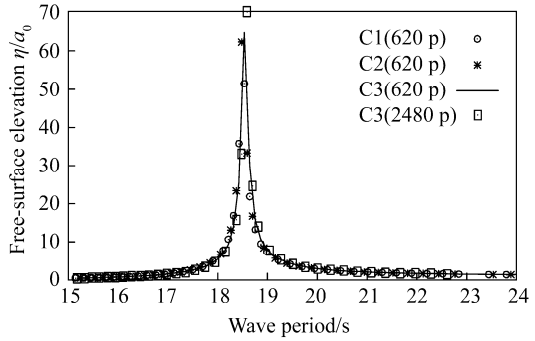

Fig.4 Results of MDBEM with different meshes

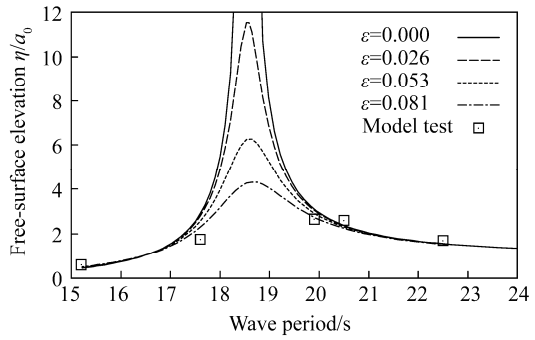

Fig.5 Results with different dissipations

6 Conclusions

A new boundary element method based on the Green integral representation of velocity potential in two separated fluid subdomains between which a control surface plays the role of interface is summarized in the paper. The integral equations of this MDBEM are established as (20) and are completed by the continuous conditions of potential and its normal derivative across the control surface. The use of MDBEM in the computation of water-column motion in a moonpool shows that it provides convergent and accurate results.

The introduction of a dissipation force in fluid decreases the resonant motions in the small zone near the resonant period. A good choice of a dissipation coefficient which may be determined by model tests or CFD computations yields results very close to those found in physics.

The MDBEM presented here for two subdomains can be easily generated in a case with more than two subdomains. Furthermore, the control surface between subdomains can be defined in an appropriate way following the properties of the problem. In particular, the introduction of additional dissipation across the control surface can be realized and has wide application potential in offshore industries.

References

Guével P (1982). *Le problème de diffraction-radiation-Première partie: Théorèmes fondamentaux*. ENSM, Univ. Nantes.

Chen XB (2004). Hydrodynamics in offshore and naval applications-Part I. *Keynote Lecture of 6th Intl Conf HydroDynamics*, Perth, Australia.

Molin B (2001). On the piston and sloshing modes in moonpools. *Journal of Fluid Mechanics*, **430**(1), 27-50.

Newman J (2003). Low-frequency resonance of moonpools. *Proc.18th IWWWFB*, Carry-Le- Rouet, France.

Sadó Garriga O, Falzarano JM (2004). Water waves and marine structure interaction. *Proc. 23rd OMAE*, Vancouver, Canada, 1155-1165.

Dai YS, Duan WY (2008). *Potential flow theory of ship motions in waves*. The National Defense Industries Press, Beijing, China.

Martin PA, Risso FJ (1993). Boundary integral equations for bodies of small, but finite, thickness. *Proc. 8th IWWWFB*, St John's, Canada.

Xiaobo Chen was born in 1961. Being Head of Hydrodynamic & Mooring Section in Research Department and Director of International R&D Cooperation of Bureau Veritas, he is involved in Professorship of Harbin Engineering University and Adjunct Professor of The University of Western Australia. His research interests are focused on ship and offshore structure hydrodynamics.

Wenyang Duan was born in 1967. He is a professor and a PhD supervisor at Harbin Engineering University. His current research interests include nonlinear wave-body interactions and the SPH method.